On the Modelling and Evaluation of Harmonic Tags

Andrei Mogilnikov and Anastasia Lavrenko
Radio Systems Group, University of Twente, 7400 AE Enschede, Netherlands (a.mogilnikov@utwente.nl)

***Abstract*—Passive harmonic tags are used to detect and track targets in highly cluttered environments or when the object of interest is too small to fit an active transmitter. This paper presents an approach to analytically model tag performance based on its equivalent circuit model. Tested on wire-based tags, it shows good correspondence with measurement results.**

I. Introduction

Harmonic tags are simple passive RF transponders used in a variety of applications ranging from insect tracking to vital sign detection [1]. Consisting of an antenna(s), a nonlinear device, and a simple matching network, a typical harmonic tag operates by accepting part of the transmitted power at some fundamental frequency f_0 (P_{in,f_0}) and generating a nonlinear return signal that contains a mix of signal harmonics. Usually, the signal power at the second harmonic ($P_{\mathrm{out},2f_0}$) is the largest so that the tag is tuned to re-transmit a signal at $2f_0$. Tag performance is therefore most commonly evaluated by its conversion efficiency, which is defined as

$$\eta = P_{\mathrm{out},2f_0} - P_{\mathrm{in},f_0},\ [\mathrm{dB}]. \tag{1}$$

Several analytical models of harmonic tags can be found in the literature [2]–[4]. However, all of them have limitations. For instance, the models in [2], [3] are based on small-signal approximations and cannot describe the tag behaviour at higher incident power [5]. On the other hand, the solution presented in [4] is based on a highly simplified circuit model that does not account for the impedance mismatch between the antenna and the diode. In this paper, we present an analytical model that rectifies these shortcomings and corresponds well with measurement results in a wide range of incident power.

II. Circuit Models of Harmonic Tags

In its simplest form, a harmonic tag is an antenna connected to a low-voltage diode. A common antenna choice in harmonic tags is a wire dipole with a small inductive loop connected in parallel to the antenna port, as schematically shown in Fig. 1.

For circuit analysis, an antenna can be represented as a Thévenin voltage source connected to the antenna's impedance $Z_{\mathrm{a}} = R_{\mathrm{a}} + jX_{\mathrm{a}}$. When the tag receives an input signal $s(t)$ at a fundamental frequency f_0, the source generates a voltage

$$V_a = \sqrt{2\ P_{\mathrm{in},f_0}\ G_{f_0}\ R_{\mathrm{a},f_0}} \cdot s(t), \tag{2}$$

where G_{f_0} is the antenna gain at f_0. A typical *p-n* junction diode can be modelled as a non-linear resistance R_{j} connected in parallel with a junction capacitance C_{j}. When the latter is low, the current generated by the diode can be described by the principal branch of the Lambert function $W_0(\cdot)$ [4]

$$I_{R_{\mathrm{j}}}(V_{\mathrm{a}}) = I_s \left[W_0\left(\rho e^{\rho + V_{\mathrm{a}}/(nV_{\mathrm{t}})}\right)/\rho - 1 \right], \tag{3}$$

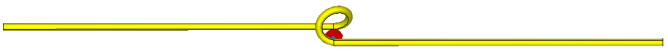

Fig. 1: Model of a wire-based harmonic tag with an inductive loop. A diode is attached in the air gap between the dipole arms.

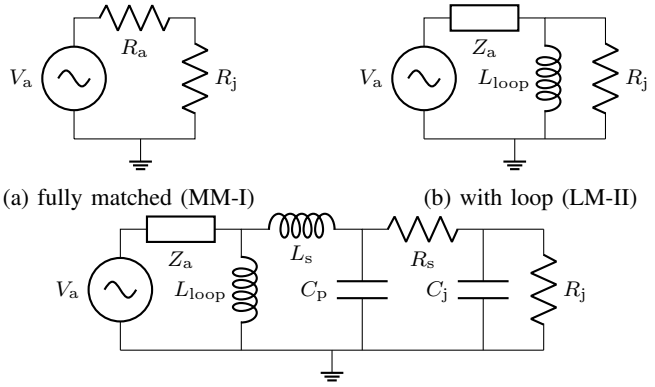

(a) fully matched (MM-I) (b) with loop (LM-II)

(c) extended (EM-III)

Fig. 2: Equivalent circuit models of a passive harmonic tag.

where I_{s} is the diode saturation current, n is the diode ideality factor, $V_{\mathrm{t}} \approx 25$ mV is the thermal voltage and ρ is a variable that depends on the circuit parameters. The power re-radiated by the tag at the second harmonic is then equal to

$$P_{\mathrm{out},2f_0} = 0.5\beta\ I^2_{\mathrm{j},2f_0}\ R_{\mathrm{a},2f_0}\ G_{2f_0}, \tag{4}$$

where $I_{\mathrm{j},2f_0}$ is the second-harmonic current generated by the diode, β is the current division coefficient, and $R_{\mathrm{a},2\mathrm{f_0}}$ is the antenna resistance at $2f_0$.

When the tag antenna is fully matched to the diode, the tag can be represented by the antenna resistance R_{a} connected to the junction resistance R_{j} (Fig. 2a). Then, $\beta = \beta^{\mathrm{I}} = 1$ and

$$\rho^{\mathrm{I}} = I_{\mathrm{s}} R_{\mathrm{a},f_0}/(nV_{\mathrm{t}}). \tag{5}$$

Matching between the antenna and the diode is often done by connecting an inductive loop in parallel to the antenna and the diode (Fig. 2b). To account for its inductance L_{loop}, the variables ρ and β should be modified as

$$\rho^{\mathrm{II}} = I_{\mathrm{s}} Z'_{\mathrm{a},f_0}/(nV_{\mathrm{t}}), \tag{6}$$

$$\beta^{\mathrm{II}} = Z_{\mathrm{loop},2f_0}/(Z'_{\mathrm{a},2f_0} + Z_{\mathrm{loop},2f_0}), \tag{7}$$

where $Z'_{\mathrm{a},f} = (Z^{-1}_{\mathrm{a},f} + Z^{-1}_{\mathrm{loop},f})^{-1}$ and $Z_{\mathrm{loop},f} = j2\pi f L_{\mathrm{loop}}$.

In practice, one also needs to account for the parasitic elements and the current going through C_{j}. The effect of diode packaging can be modeled as a series inductance L_{s}, a shunt capacitance C_{p}, and a contact and current-spreading series resistance R_{s} (Fig. 2c). In this case,

$$\rho^{\mathrm{III}} = I_{\mathrm{s}} Z''_{\mathrm{a},f_0}/(nV_{\mathrm{t}}), \tag{8}$$

TABLE I: Diode SPICE parameters

Parameters		SMS7630	SMV2019
Saturation current	I_s, A	5e-6	1e-14
Junction capacitance	C_j0, pF	0.14	2.25
Built-in voltage	Φ, V	0.34	3.5
Series resistance	R_s, Ω	20	4.8
Profile parameter	M	0.4	1.4
Ideality factor	n	1.05	1
Parasitic capacitance	$\mathrm{C_p}$, pF	0.16	0.07
Series inductance	L_s, nH	0.7	0.7

TABLE II: Tag parameters at f_0 = 2.9 GHz

Parameters		Tag A	Tag B	Tag C
Diode model		SMS7630	SMS7630	SMV2019
Diode impedance, Ω	f_0	$10.7 - j170.4$		$4.5 - j10.9$
	$2f_0$	$5.9 - j66.3$		$4.5 + j13.6$
Joint impedance $Z'_{\mathrm{a},f}$, Ω	f_0	17.8 + j41.5	29.2 + j50	
	$2f_0$	13.5 + j147	37.4 + j244	

where $Z''_{\mathrm{a},f} = R_\mathrm{s} + [Z^{-1}_{\mathrm{Cp},f} + (Z_{\mathrm{L_s},f} + Z'_{\mathrm{a},f})^{-1}]^{-1}$, $Z_{\mathrm{Cp},f} = (j2\pi f C_\mathrm{p})^{-1}$ and $Z_{\mathrm{L_s},f} = j2\pi f \mathrm{L_s}$. To find $I_{\mathrm{j},2f_0}$ one now needs to sum the current through the junction resistance and the junction capacitance. The current division coefficient then becomes

$$\beta^{\mathrm{III}} = \beta^{\mathrm{II}} \frac{Z_{\mathrm{Cp},2f_0}}{Z'_{\mathrm{a},2f_0} + Z_{\mathrm{L_{s,2f_0}}} + Z_{\mathrm{Cp},2f_0}} \frac{Z_{\mathrm{j},2f_0}}{Z''_{\mathrm{a},2f_0} + Z_{\mathrm{j},2f_0}}, \quad (9)$$

where $Z_{\mathrm{j},f} = (R^{-1}_{\mathrm{j},f} + j2\pi f C_\mathrm{j})^{-1}$.

III. Experimental Verification

We tested presented analytical models with three wire-based tags. Each had a half-wavelength (at $f_0 = 2.9$ GHz) dipole antenna made from a copper wire (diameter 0.5 mm, G_{f_0} = 2.1 dBi, G_{2f_0} = 3.9 dBi) with a diode (SC-79 packaging) and a circular inductive loop in the middle. The tags differed from each other by the diode model and the diameter of the loop (see Tables I and II for diode and tag parameters, respectively).

The wire tags were measured inside an anechoic chamber with transmitting and receiving antennas placed 1.5 m above the ground and the tags positioned in front of them at a distance of 40 cm. The incident carrier signal was generated by a signal generator (Agilent E8267D), amplified by a custom power amplifier (PA) (Storz consulting, 25 dB @f_0) and transmitted through a logarithmic periodic antenna (LP WA5VJB, 4.2 dBi @f_0). Furthermore, a low-pass filter (Mini Circuits VLP-3800+, -38 dB @$2f_0$) was connected to the PA output port to suppress parasitic harmonics. Taking into account cable and propagation losses, this resulted in an incident power level P_{in,f_0} that extended the range from -30 to 3 dBm. The signal re-radiated by the tag at $2f_0 = 5.8$ GHz was measured by a spectrum analyser (SA) (Agilent E4404B) using a helical antenna (Heliaxial58, 12 dBi @ $2f_0$). SA settings provided a noise floor less than -123 dBm.

Fig. 3 compares the measured tag conversion efficiency η with the results provided by the three models considered above: fully matched model (MM-I), loop model (LM-II), and extended model (EM-III). For all three tags, MM-I [4] provides an implausibly high evaluation of η since it does not account for the mismatch between the antenna, loop, and the diode. Including the loop into the model in LM-II enables a

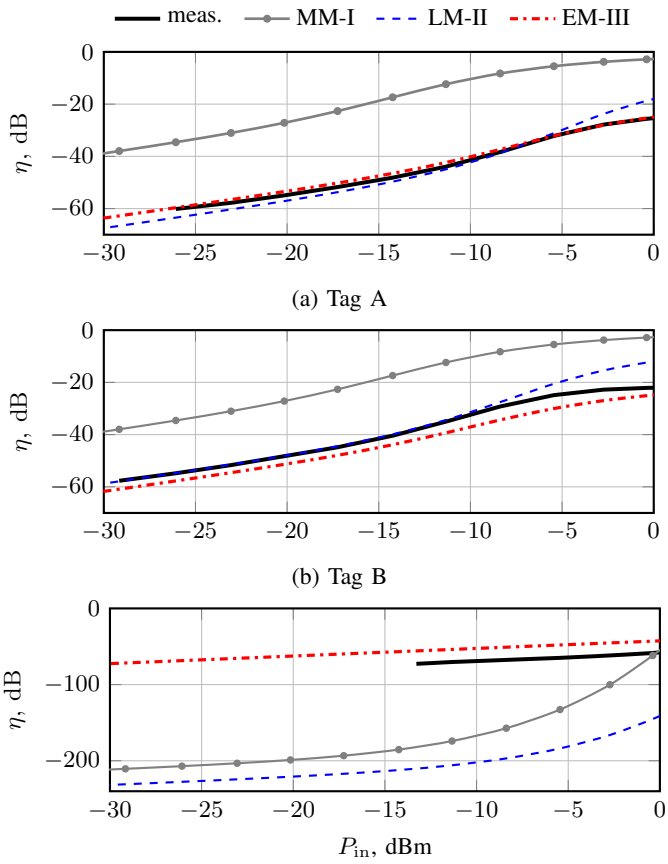

(a) Tag A

(b) Tag B

(c) Tag C

Fig. 3: Comparison of the measured conversion efficiency η of the tags with the simulation results at $f_0 = 2.9$ GHz.

much closer prediction of tag performance for Tags A and B that have the same diode (Schottky diode SMS7630) but different loop sizes. However, it still fails dramatically for Tag C. The reason is that SMV2019 is a varactor diode that has a significantly higher C_j and a much lower I_s than a Schottky diode. Extending the model to directly include C_j and diode parasitics enables a higher accuracy in estimating η. Applied to Tags A and B, EM-III also provides a better fit at higher input power.

Acknowledgement

The authors are grateful to R. J. de Jong and Z. Mahfouz for their help with the tag manufacturing and measuremens.

References

[1] A. Mishra and C. Li, "A review: recent progress in the design and development of nonlinear radars," *Rem. Sens.*, vol. 13, no. 24, 2021.

[2] K. Rasilainen, J. Ilvonen, A. Lehtovuori, J.-M. Hannula, and V. Viikari, "On design and evaluation of harmonic transponders," *IEEE Trans. on Antennas and Propag.*, vol. 63, no. 1, pp. 15–23, 2014.

[3] X. Gu, N. N Srinaga, L. Guo, S. Hemour, and K. Wu, "Diplexer-based fully passive harmonic transponder for sub-6-GHz 5G-compatible IoT applications," *IEEE Trans. Microw Theory Tech.*, vol. 67, no. 5, pp. 1675–1687, 2018.

[4] A. Lavrenko and J. Cavers, "Two-region model for harmonic radar transponders," *Electronics Letters*, vol. 56, no. 16, pp. 835–838, 2020.

[5] M. Polivka, V. Hubata-Vacek, and M. Svanda, "Harmonic balance/full-wave analysis of wearable harmonic transponder for IoT applications," *IEEE Trans. on Antennas and Propag.*, vol. 70, no. 2, pp. 977–987, 2021.